Electronic Structure Theory of Radiation-Induced Defects in Si/SiO_2

Andrew C. Pineda[†] and Shashi P. Karna[‡]

[†]*Albuquerque High Performance Computing Center, The University of New Mexico, 1601 Central Avenue, NE, Albuquerque, NM 87131*

[‡]*US Air Force Research Laboratory, Space Vehicles Directorate, 3550 Aberdeen Ave, SE, Bldg. 914, Kirtland AFB, NM 87117-5776*

ABSTRACT

Radiation-induced defects in metal-oxide semiconductor (MOS) materials are a major problem for MOS devices exposed to high-energy radiation such as in space-based applications. Charge trapping at these defect sites degrades the current/voltage performance of MOS devices and ultimately leads to device failure. A physical understanding of the structure and formation mechanisms of these defects is becoming increasingly important as the size of these devices continues to decrease. Because these defects are highly localized, *ab initio* quantum chemical methods applied to model clusters have been very successful in providing insight into their local structure as well as physical properties such as electron spin resonance (ESR) spectra. They also give insight into the formation mechanisms of these centers. Of interest to us is the identification and characterization in amorphous silicon dioxide (a-SiO_2) of what are collectively known as E' centers. These centers all appear to be characterized by an unpaired electron that is strongly localized on the dangling sp^3 orbital of a Si atom that is bonded to three O atoms.

We report *ab initio* Hartree-Fock calculations that we have performed on possible models for oxygen vacancy sites: a 5-Si center, a 4-Si center, and a 2-Si center model. Clusters of increasing size and flexibility are used to verify that the properties that are computed are insensitive to the sizes of the clusters that are used. They are also used to demonstrate the effects of SiO_2 network flexibility on the mechanism of defect formation. The clusters employed in these studies ranged from 28 to 87 atoms in size. These calculations were performed using STO-3G and DZP (Double zeta+polarization) basis sets and are only made possible by the availability of high performance computing resources.

Our calculations confirm the previous work of Chavez, et al.[1] that the E'_δ center, characterized by a nearly isotropic 100G hyperfine splitting, is a positively-charged symmetrically-relaxed 2-Si center in which the unpaired electron is equally shared by the two Si atoms. Another center, characterized by a 420G hyperfine splitting and known as the E'_γ center, is believed to be a positively-charged and asymmetrically-relaxed 2-Si center in which the unpaired electron is localized on one of the Si atoms and the positive charge on the other Si. This model, in which the positively charged Si atom is stabilized by forming a bond with an O atom (which becomes 3-fold coordinated) from the surrounding SiO_2 network, was first proposed by Feigl, Fowler, and Yip[2] for a similar defect known as the E_1 center in α-quartz. Formation of E'_δ or E'_γ centers by hole trapping at 2-Si vacancy centers is found to be determined by the flexibility of the local SiO_2 network. This stands in contrast to the prior work using semi-empirical and DFT methods that have suggested that the symmetrically relaxed and asymmetrically relaxed configurations are bistable minima. No evidence of bistability is found in our calculations.

INTRODUCTION

In this paper, we review some of the research by our group over the past few years into the electronic structure[1, 3] and formation mechanisms[4] of point defects in amorphous SiO_2 (*a*-SiO_2). The primary focus of these studies has been a class of defects known as the E′ centers. The E′ centers are perhaps the most extensively studied point defects in *a*-SiO_2[5,6] and belong to a family of five positively charged defect centers identified to date in thin SiO_2 films.[7,8] The E′ centers, as identified via electron spin resonance (ESR) spectroscopy, are associated with an unpaired electron centered on (a) a single Si atom adjacent to vacant oxygen (V_O) sites or (b) on multiple Si atoms within the region containing excess Si centers (ESC) or Si "islands" in the oxide network. Similarly, triplet centers, with two unpaired electrons, are also believed to be associated with vacancy sites. These centers are believed to be the primary hole trap centers in the metal-oxide-semiconductor (MOS) devices[9,10] where they affect electrical properties such as leakage currents, current-voltage (I/V) behavior, and ultimately device reliability. Although the exact mechanism of hole trapping by oxygen vacancy sites remains unknown, it is widely accepted that network relaxation leading to the creation of deep trap levels in the SiO_2 band gap is one of the consequences of charge trapping. The latter phenomenon causes a long-term build up of oxide-trapped positive charge. However, the exact nature of the network relaxation that results in the long term build up of oxide charge following charge trapping remains unknown to date. The deleterious effect of this charge buildup on device behavior has become much more significant as semiconductor devices have decreased in size. Therefore, the development of an understanding of the microscopic structure, stability,

formation mechanisms, and electrical characteristics of these centers have been the focus a great deal of attention over the past decade.

Microscopic structure of defect centers

Among the various flavors of the E′ centers in *a*-SiO_2, the E'_γ center appears to be the most common high-energy radiation-induced oxygen vacancy center generated in oxides prepared under a variety of conditions. The characteristic features of the ESR spectrum of the E'_γ center are: (a) a 420 G splitting in the hyperfine spectrum and (b) an anisotropic g-tensor (g_{11}=2.0018, g_{22}=2.0006, g_{33}=2.0003). Extensive experimental[11-13] and theoretical studies, [2,14-16] performed in the past, have identified this center as a pair of silicon atoms, one bearing an unpaired electron spin and the other bearing a positive charge, adjoining an oxygen vacancy site ($Si^{\uparrow}$—Si^{+}). The unpaired electron is localized primarily on an sp^3 bonding orbital of a tetrahedral Si. The positively charged Si atom is far removed from its tetrahedral counterpart and believed to be bonded to a triply coordinated O atom in the oxide network. From the point of view of the ESR experiment, the important feature of this center is that the unpaired electron spin is localized on a single Si atom.

In contrast to the E'_γ center, which has been known for over 30 years, the E'_δ center has been detected only recently. This center was first detected by Griscom and Frieble[11] in 100 keV x-ray irradiated bulk silica containing a high density of chlorine impurity. Later, it was also detected in γ-ray irradiated high purity silica glasses.[17] Vanheusden and Stesmans[18] detected this center in buried oxide (BOX) layers formed by O^+ implantation during the separation by implantation of oxygen (SIMOX) process. Similar observations have been reported by Warren et al.[19] In recent years, this center has also been detected in the thermally grown oxide films upon annealing [20-24] and in x-ray irradiated high purity

silica glass.[25] The characteristic features of the E'_δ centers are (a) a 100 G doublet hyperfine splitting, and (b) a nearly isotropic g-tensor (g_{11}=2.0018, g_{22}=2.0021, g_{33}=2.0021) in the electron spin resonance (ESR) spectrum.[11,25] The hyperfine splitting and the g-tensor are attributed to ^{29}Si centers in the oxide samples.[11,18,19,25] Another important feature of this center, as observed from the ESR spectrum of irradiated glass samples,[11,17,25] is the simultaneous appearance of a triplet state spectrum. The charge state of E'_δ is believed to be positive.[18,19]

While the total spin and the charge state of the E'_δ center extracted from the ESR and the electrical measurements are believed to be well established, the exact nature of its microscopic structure has been the subject of considerable debate. Analysis of the ESR spectrum for this center, vis-à-vis that of the more extensively studied E'_γ center in *a*-SiO_2,[5-13] suggests that the unpaired electron spin in the E'_δ center is delocalized over four, nearly equivalent, Si atoms. Since *a*-SiO_2 is a network of tetravalent Si atoms connected via divalent bridging O atoms, an atomic arrangement with four equivalent Si atoms requires multiple-oxygen vacancies or domains of unoxidized, tetrahedrally-connected Si atoms, also referred to as oxygen deficient centers (ODCs), in the oxide. These arguments have led a number of groups to propose multiple-oxygen vacancy models. For example, Griscom and Frieble[11] proposed a model in which the unpaired electron spin is delocalized over four tetrahedral bonds of equivalent but different Si atoms. The model proposed by Vanheusden and Stesmans[18] and Warren et al.[19] involves delocalization of the unpaired electron spin over four equivalent Si atoms connected to a central tetrahedral Si atom (the *five-Si atom model*).

In contrast, the model proposed by Zhang and Leisure[25] involves delocalization of the electron spin over four equivalent Si atoms around a SiO_4 vacancy (the *four-Si atom model*). In addition to the multi-oxygen vacancy models, mono-oxygen vacancy models have also been proposed in the literature[17,21] to describe the local atomic configuration of the E'_δ center. In these models, the unpaired electron spin is believed to be localized either on a Si-Si dimer[17] or on a single Si atom[21] as in the case of the E'_γ center (the *two-Si atom model*).

The triplet state species with two unpaired electrons having parallel spins (total spin, S=1, spin multiplicity, M_s=3) have only been detected in irradiated bulk silica samples.[11,17,22] The triplet-state center has a number of very interesting properties. For example: (a) it always appears in the samples where E'_δ is observed; (b) it is observed in the samples which exhibit a 5 eV absorption followed by a 4.4 eV photoluminescence; (c) it is only found in low-OH oxygen-deficient samples with no Cl impurity; and (d) its ESR properties (a nearly isotropic g-value=2.002 and a hypefine splitting of 134 G) are strikingly similar to those of the E'_δ center. Furthermore, its annealing behavior is also very similar to that of the E'_δ center. Previous workers have suggested[11,17,25] that the two paramagnetic centers may have common local atomic structure due to the observed similarities in the properties of the triplet-state and the E'_δ centers.

An initial attempt to establish the microscopic structure of these defects in *a*-SiO_2 via quantum mechanical calculations was the study by Chavez et al.[1] of the E'_δ center. They examined the proposed atomic models for the E'_δ center[14,18,25] by *ab initio* Hartree-Fock (HF) calculations of the stable geometry, energy, and spin properties of model clusters. Their calculations suggested that subsequent to the hole trapping, the free electron

spin prefers to localize on a pair of Si atoms regardless of the number (five, four, or two) of Si atoms around oxygen vacancy.[1] Furthermore, the calculated spin density and the hyperfine coupling tensor on the two participating Si atoms showed excellent agreement with the experimental ESR data. From these results, they concluded that the E'_δ center most probably resulted from an equal distribution of the unpaired electron spin over two equivalent Si atoms and suggested that the E'_δ center was a symmetrical variant of the E'_γ center.[1] In the latter case, the spin is asymmetrically localized on a single Si center around a mono-oxygen vacancy.

Since Chavez et al.[1] used relatively small atomic clusters to model the E'_δ center, it was not clear if the size of the clusters had any influence on the calculated results for the spin density. They also did not study the triplet-state centers.[1] In view of the importance effects of oxygen vacancy related point defects on the reliability of MOS devices, we have performed *ab initio* HF calculations on the E'_δ centers employing extended sets of atomic basis functions and much larger model cluster structures. Because of their size, these calculations require the use of high performance parallel computing resources. We have performed similar calculations on the triplet-state centers employing somewhat smaller clusters. The results for the E'_δ centers[1,3] using clusters of different sizes are all consistent with one another suggesting that the observed ESR spectrum results from an unpaired electron distributed over a pair of Si atoms arranged around a mono-oxygen vacancy. The calculated results for the ESR hyperfine coupling tensor for model triplet-state structures are too large compared with the experiment.[11,17,25]

Hole trapping mechanism

According to a popular model, proposed by Feigl, Fowler, and Yip[2] (FFY) a quarter of a century ago, trapping of a hole by an oxygen vacancy site in α-quartz causes an asymmetric relaxation of the Si atoms adjacent to the vacancy. Specifically, the hole is localized on a silicon atom that moves away from its original position in the vacancy through the plane of its three adjoining oxygen atoms where it is stabilized by bonding to an oxygen atom from the surrounding network while an unpaired electron is localized on another three-fold coordinated silicon atom that essentially remains fixed at its original position in the vacancy. The unpaired electron occupies one of the dangling sp^3 bonds of the undisplaced silicon atom. This model, which was originally proposed to explain the observation of electron spin resonance (ESR) detection of an oxygen vacancy center in α-quartz known as the E'_1 center, is widely used to explain the formation mechanism and local atomic structure of the related E'_γ defect center in *a*-SiO_2. Although it has not been verified experimentally to date, the most appealing feature of the FFY model lies in its ability to provide a physical basis to explain the localization of the unpaired electron spin following hole trapping on a single silicon atom, as evidenced from the ESR spectrum of the E'_γ center.

The FFY model is supported by quantum mechanical semi-empirical calculations within the cluster approach[26] and density functional theory (DFT) calculations within the supercell approach[27] which suggest that upon hole trapping, an oxygen vacancy relaxes asymmetrically with a lowering of the total energy of the system by about 0.3-0.4 eV. The DFT calculations also suggest that the asymmetric relaxation of the network does not occur

spontaneously after hole trapping by an oxygen vacancy, but rather the process involves an energy barrier of about 0.1-0.4 eV.[27]

Despite its widespread appeal, the FFY model fails to explain a number of important features related to charge trapping at an oxygen vacancy in *a*-SiO_2, or its charge state. One such example is the ESR observation of the E'_δ center.[11,17,18,24,25] Our group's *ab initio* quantum mechanical calculations,[1,3] performed on model SiO_2 clusters, have established this center to be a hole trapped at a simple mono-oxygen vacancy site. The E'_δ center results from a hole trapped at an oxygen vacancy site in which the unpaired electron spin is shared equally by two silicon atoms. The hole trapping in this case causes a "symmetric relaxation" that leads to a slight increase in the internuclear distance between the two Si atoms adjacent to the relaxed neutral oxygen vacancy. This suggests that asymmetric relaxation of the SiO_2 network is not the only effect caused by hole trapping at an oxygen vacancy center in *a*-SiO_2.

The FFY model also fails to describe the neutral E' centers, also known as hemi-E' (E'_h) centers, in *a*-SiO_2.[28-30] Their ESR features, including the characteristic resonance position of the spectrum, the g-tensor, and the electron spin - nuclear spin hyperfine coupling tensor, are remarkably close to those observed for the E'_γ centers. The experiments and *ab initio* quantum mechanical calculations agree on the fact that the unpaired electron is localized on a dangling sp^3 bond at a three-fold coordinated silicon center. It is therefore not clear whether hole trapping is a necessary condition for the observation of the so-called E'_γ centers, since the charge states of these defects have never been established unambiguously.

In light of these facts, it is important to develop an improved understanding of the microscopic effects of charge trapping by oxygen vacancy centers in *a*-SiO_2. It is clear, however, that the present model of the charge trapping by an oxygen vacancy does not fully account for all known effects. Therefore, it is important to develop a more comprehensive understanding of the effect of charge trapping by oxygen vacancy sites in *a*-SiO_2. In order to gain such an understanding, we have performed *ab initio* Hartree-Fock calculations on model SiO_2 clusters of varying size and geometrical features. Attention is focused on (a) the energy of oxygen vacancy formation, $\Delta E_f(V_O)$, in the neutral and positive charge state and (b) changes in the structural features following hole trapping by an oxygen vacancy.

Our results suggest that both $\Delta E_f(V_O)$ and the structural changes for neutral and positively-charged oxygen vacancies depend upon the starting local structure of the SiO_2 network. The technical details of the calculations are described in the following section. Subsequently, the results of the calculation are presented and discussed. The main findings of the study are then summarized in the conclusion.

CALCULATIONS

The model clusters used in the studies that we report on are shown in Figures 1 through 4. Model A represents a defect consisting of an island of five Si atoms. Shown in **Figure 1a** is the optimized structure of the neutral model A. Model B, shown in **Figure 1b**, represents a defect consisting of an island of four Si atoms. It was derived from model A by removing the central Si atom. Model C, shown in **Figure 2a**, is the simplest possible precursor for a 2-Si vacancy center. Model D is derived from model C by removing the bridging O atom. Model E, shown in **Figure 3a**, is a larger precursor (39 atoms) for a 2-Si

vacancy center and model F, shown in **Figure 3b,** is the corresponding vacancy. Model cluster E consists of two fused pairs of six-atom rings with alternating Si—O bonds (or in the parlance of the solid state community, fused pairs of three-member rings where "member" refers only to the number of silicon atoms in the rings) bridged by a single oxygen atom. Model F was generated by removing a bridging O atom from the neutral oxide cluster, model E. Model G, shown in **Figure 4a,** is the largest precursor cluster (87 atoms) used in our study. It consists of two fused pairs of twelve-atom (six-member) rings bridged by a single oxygen atom. Models H and I, were generated from model G by removing the bridging oxygen atom and optimizing the structures in the neutral (**Figure 4b**) and positive charge (**Figure 4c**) states, respectively. The largest spheres, colored black, in the figures represent the Si atoms, the medium-sized spheres, in red, represent the O atoms and the small outer spheres, in white, represent H atoms. The H atoms were used to saturate the valency of the outer O atoms.

In what follows, we will also refer to oxygen vacancy sites derived from a particular precursor, X, as $V_O^q(X)$, where *q* denotes the charge of the site. This notation is more convenient for some discussions as well as in the tables and figures.

The total energy and the spin density of the positively charged clusters were calculated by the *ab initio* unrestricted Hartree-Fock (UHF) method. For the neutral clusters, properties were calculated using the restricted Hartree-Fock (RHF) method. A double zeta Cartesian Gaussian basis set augmented by a six-component *d* polarization function on Si and O atoms and a three-component *p* polarization function on the H atoms (DZP basis set) was used in most calculations. Where noted below, a minimal (STO-3G) basis set was also used in some calculations. Calculations were performed using the

GAMESS[31] and HONDO[32] *ab initio* electronic structure codes on a wide variety of computational platforms. The former was used for total energy and spin density calculations as well has geometry optimizations. The latter was used for the calculation of ESR hyperfine coupling constants. All atoms were allowed to move in the geometry calculations.

Computational Aspects of Our Calculations

Of the two *ab initio* codes used in our calculations, only the GAMESS code has been parallelized. While we have not yet performed a quantitative analysis of the behavior of GAMESS in our research, we feel that some qualitative comments about our experiences with the code are worthwhile.

In this work, we have used several versions of the GAMESS code beginning with the January 6, 1998 release and continuing through the June 1999 release. We have also used the GAMESS code on a number of computational platforms including a variety of IBM SP2's (66MHz P2 thin nodes at the Albuquerque High Performance Computing Center, 66MHz P2 thin nodes and 160MHz P2SC thin nodes at the Maui High Performance Computing Center, and similar nodes at the Aeronautical Systems Center), SGI Origin 2000's (at AHPCC and ASC), and a 64-node Linux-based Dual Pentium II 450 MHz SMP Superclusters (at AHPCC) using Myrinet-based communications.

More recently, we have been using Linux Superclusters with either Myrinet-based or Gigabit Ethernet-based communications, CPU speeds from 450MHz to 550MHz, and 2 to 4 processors per node. Among the issues we are facing with running such large problems these new platforms are what we suspect are memory allocation problems within communications driver routines. Debugging these problems is made challenging by the fact that errors crop up only after the code has been running for many hours.

Another difficult challenge in performing these calculations is that the time required for many calculations, especially the job queues, usually exceeds the maximum time limits of the batch queues at most high performance computing centers. A rough indication of the typical requirements is provided by **Table 1** where we give some data on the total amount of processing power used in studying the various model clusters appearing in this work.

A detailed analysis of the performance of the GAMESS code on Linux-based SMP Superclusters is currently being undertaken at the AHPCC. We hope to report on this study at the next DoD User Group meeting.

Calculations to identify the structure of the E'_δ and triplet centers

In order to identify the local structure of the E'_δ center, the properties of models A, B, and F were computed in the positive charge state (q= +1). Calculations on model A were performed at the *ab initio* HF optimized equilibrium geometry of the neutral cluster (q=0). Calculations on model F were performed at the *ab initio* HF optimized geometry of the neutral oxide cluster (Model E).

For the two-Si center model (model C), the ESR hyperfine coupling constants were also calculated using a minimal (STO-3G) and a double-zeta valence (DZP) basis set.

As explained below, the calculations on the triplet-state centers were performed on two-Si atom model (model D) only.

Calculations examining formation mechanisms of oxygen vacancy centers

Precursor Calculations

The precursor clusters used to generate the model mono-oxygen vacancy clusters in the present study are the topmost clusters shown in Figures 2 through 4. Model C (**Figure 2a**) is the simplest model for a two silicon center while clusters E and G essentially model Si—O networks of increasing size and flexibility. The optimized atomic configurations of

the neutral precursor clusters C and E were taken from our previous studies.[1,3] The optimized geometry of the precursor cluster G was obtained by a RHF calculation using a minimal (STO-3G) basis set.

Charged and Neutral Mono-Oxygen Vacancy Calculations

Models for neutral mono-oxygen vacancies (V_O^0) were generated by removing the bridging oxygen atom connecting the two central silicon atoms in the precursor clusters and then optimizing the resulting structures via an *ab initio* RHF calculation. As in the precursor case, the small and medium neutral vacancy models, V_O^0(C) and V_O^0(E), were optimized using a DZP basis set and the large neutral model cluster, V_O^0(G), was optimized using a minimal (STO-3G) basis set. Positively charged mono-oxygen vacancies (V_O^{+1}) were similarly generated by removing the bridging oxygen atom and an electron, and then optimizing the resulting structures via an *ab initio* unrestricted Hartree-Fock (UHF) calculation using the same basis sets.

Distortions of the neutral and positively charged vacancies about their respective equilibrium atomic configurations were also studied by adding or removing an electron to the optimized positive and neutral vacancies and optimizing the structures again. If no spontaneous relaxation of the positively charged cluster occurred in the course of the geometry optimization, then a silicon atom from the vacancy was moved into the adjoining network in order to attempt to locate a second energy minimum. The specific details of these calculations will be discussed on a case by case basis in the next section.

RESULTS

Structure of the E′ center:

The five-Si atom model (model A).

The Si—Si bond distances in the neutral model A (**Figure 1a**) cluster are calculated to be between 2.350 Å and 2.362 Å and the calculated Si—O bond distances range from 1.628 Å to 1.630 Å, in good accord with the literature data.[1] The bonds at the central silicon atom are very nearly equivalent to each other as is noted from the Si_o—Si_c—Si_o bond angles which range between 109^0 and 111^0. The subscript *c* indicates *central* and *o* indicates *outer*. The equivalence of the outer four Si atoms is also noted from the Mulliken population analysis, which gives a net charge between 1.428389 and 1.449943 for the outer Si atoms. When a hole (q = +1) is placed on this cluster, the net calculated charge on the outer Si atoms is calculated to be between 1.486277 and 1.508052. The total spin density, ρ^0, (the excess of α over β spins) calculated for the outer four Si atoms are: -0.003626, 0.175657, 0.053748, 0.013128. While the net atomic charges on the Si centers are not too different from each other, the corresponding spin densities differ greatly. It is clear that the spin density is not equally distributed on the outer four Si atoms. Moreover, the value of the calculated spin density is too small relative to the experimental value of about 0.32[11, 25] for the E'_δ center.

The four-Si atom model (model B).

For model B (**Figure 1**), the calculated values of the spin density, ρ^0, at the four Si centers are: 1.018086, 0.993140, -0.221734, and -0.280082. Once again, it is clear that the spin density is not equally distributed over the four Si atoms. Also, the magnitudes of the calculated spin densities are vastly different from the experimental value.[11,17,25] However, the spin density seems to be distributed on a pair of equivalent Si atoms.

The two-Si atom model (model F,V_O^+(E)).

For model F (**Figure 3b**), the calculated spin density, ρ^0, at the two Si atoms are 0.304606 and 0.335135. These values are in good agreement with experiment[11,17,25] and the previously reported theoretical values.[1] The calculated value of ρ^0 on the first nearest neighbor O atoms varies from a low of 0.04 to a high of 0.06. Similarly, the spin density, ρ^0, at the second nearest neighbor Si atoms is calculated to have a value between 0.002 and 0.005. *N*th nearest neighbor atoms (*N*>2) have still smaller values for ρ^0. This suggests that the spin density in the two-Si atom model is mainly distributed over the pair of Si atoms adjacent to the oxygen vacancy.

The calculated spin properties of the two Si atoms adjacent to the O vacancy for these model structures are listed in **Table 2**. Listed in the table are the spin density, ρ^0, the isotropic hyperfine coupling constant, a_{iso}, and the principal components of the anisotropic hyperfine coupling tensor, **T**. The unit for the hyperfine coupling constant (a_{iso}, **T**) is *Gauss* (G). The spin density, ρ^0, provides information on the *s*-electron spin density at the atomic nucleus, in this case Si, and contributes directly to the isotropic hyperfine coupling constant. Electrons in the *p* and higher order angular momentum wavefunctions have zero density at the nucleus. The anisotropic hyperfine tensor, **T**, provides information on the spin density distribution away from nucleus and contains contributions from non-*s* type orbitals in the wavefunction. The measured hyperfine splitting tensor, **A** (= a_{iso}+**T**), contains contributions from the isotropic and the anisotropic part. We note from the table that the minimal basis set (STO-3G) gives somewhat lower values of ρ^0 and a_{iso} than the extended DZP basis set. However, both basis sets give comparable values for the components of **T**, this is expected. The isotropic part, which depends on the accurate

evaluation of spin density at a single point, is known to be much more sensitive to the choice of basis set than the anisotropic part.[33] The latter depends upon the spin density in the regions away from the nucleus, and can be evaluated accurately with a reasonable basis set. Accurate evaluation of the isotropic part, on the other hand, requires a highly flexible and extended basis set. This is because the standard basis sets, which try to approximate the true atomic orbitals by sums of a small number of Gaussian functions, have expansion coefficients that are chosen to minimize the error in the approximation over $r \in [0,\infty)$ and hence are a poor approximation at r=0.

We note that as the basis set improves, the calculated a_{iso} moves closer to the experimental value of 100 G.[11,17,25] In fact, the spin density, ρ^0, calculated from our DZP basis set, as discussed above, is in excellent agreement with the experimental value for the E'_δ center. We also note that the magnitude of the a_{iso} is much larger than the components of T by a factor of 5 to 10 for the DZP basis. This suggests that the wavefunction of the unpaired electron has at least a 5:1 ratio of the *s* and *p* characters. Note that the greater the *s* character in the wavefunction, the more isotropic the hyperfine coupling and the g-tensor. This may explain the observed "near isotropy" of the hyperfine splitting and the g-tensor in the ESR spectra[11,17,25] for the E'_δ center.

Structure of the triplet-state center:

Since our calculations on the E'_δ centers did not support the five-Si and the four-Si models as the microscopic structure, we excluded these models from our initial study of the triplet-state center and focused our attention on the two-Si model cluster. The reason for this selection was the assumption that the E'_δ and the triplet-state centers have common microscopic structure. As noted earlier, we used the model cluster D $[(HO)_3Si\ \ Si(OH)_3)]$

of Ref. [1] for this study. Although considerably smaller than the structures shown in **Figure 3** and **Figure 4**, this model cluster retains all the essential features of a two-Si model. The Si atoms adjacent to V_O are each bonded to three O atoms. The valency of the outer O atoms are saturated by H atoms. Property calculations were performed on two atomic configurations. The first configuration was based on that of the neutral precursor containing the middle oxygen. The first triplet state configuration was generated by simply removing the bridging O atom from the precursor cluster. This configuration, is labeled as *precursor* in the table. The other configuration, called *optimized*, was obtained from a full HF geometry optimization of the cluster without the bridging oxygen atom. This configuration represents a Si—Si dimer structure. The calculated values of Si—Si internuclear distance, the total energy, E, and the spin properties for the triplet state center in the two configurations are listed in **Table 3**. Since the two Si atoms adjacent to the oxygen vacancy in this case are exactly equivalent, the spin properties for only one center in each configuration is listed.

We note that the two Si atoms move away from each other as the structure is allowed to relax. As the Si—Si internuclear distance increases, the spin density on the Si centers decreases. However, in both configurations the calculated values of the hyperfine coupling constants are much larger than the observed value of 134 G[11,25] by a factor of four or more. Such a large difference between the calculated values of hyperfine couplings for the model structure and the experimental value for the triplet-state center rules out the possibility of the former representing the microscopic structure for the latter. This raises the question: What is the origin of the 134 G triplet observed in the ESR spectra of irradiated *a*-SiO_2? A straightforward answer to this question is not possible on the basis of

our limited study. However, it seems plausible that the E'_δ and the triplet centers do not share a common microscopic structure. One takes note of the fact that the E'_δ center is a hole (q=+1) trapped at an oxygen vacancy, while the triplet-state species is a *neutral* (q=0) center with two unpaired electrons. Therefore, the two species may have different geometrical features due to the difference in the local electronic environment. In order to further pursue this reasoning, we calculated the hyperfine properties of a four-Si cluster in which the valency of the Si atoms were terminated by H atoms. This structure, generated from a five-Si tetrahedral cluster by removing the central Si atom, was taken from our previous work.[1] The calculations were performed by an *ab initio* UHF method using a minimal (STO-3G) basis set. The calculated values of ρ^o at the Si centers are: 0.5307, 0.5232, -0.2009, 0.5216. The corresponding values for a_{iso} (G) are: -168.28, -165.99, 63.72, -165.48. In this case, the calculated spin properties of three centers are closer to the experimental value. However, one of the centers has opposite sign of the spin with much lower magnitude of the spin density. Therefore, this model can not adequately explain the observed spectrum since the four Si centers are required to be equivalent.

Formation Mechanisms of Oxygen Vacancy Centers

Information about the local structure of the precursors and optimized neutral vacancies are summarized in **Table 4** and **Table 5**, respectively. After forming the neutral vacancies from the precursors by removing the bridging oxygen atom, the two central silicon atoms in all cases moved into the vacancy site (see **Figure 2b**, **Figure 3b,** and **Figure 4b**) and formed bonds between 2.33 Å and 2.44 Å in length. These values are in good accord with literature data for a Si—Si bond.[1,34] The bond lengths for the Si—O bonds are approximately 1.6 Å for all the clusters, both neutral and charged, we have studied. As the size of the clusters increases, the range of observed Si—O bond lengths

observed increases slightly. The Si—Si bond distance in the precursors is largest in the medium-sized cluster (**Figure 3a**), probably owing to steric effects arising from the relative rigidity of that cluster. The O—Si—O bond angles in the neutral vacancy models are in general smaller than the tetrahedral bond angle of 109°, indicating that most of the decrease in distance between the silicon atoms is due to motion of the atoms adjacent to the vacancy rather than motion of the two halves of the cluster toward each other.

Information about the local structure of the optimized positively charged vacancy models are summarized in **Table 6**. When the positively charged vacancies were formed by the removal of the bridging oxygen and an electron from the corresponding precursors, different behavior was observed depending upon the availability of an oxygen atom from the surrounding network for binding and upon the flexibility of the surrounding oxide network. In the case of the small- and medium-sized, positively-charged vacancies, V_O^+(C) and V_O^+(E), the two central silicon atoms also move into the vacancy site, again forming a dimer, albeit with a longer bond distance on the order of 2.7 Å. The spin density on the central silicon atoms remains approximately equal, indicating that the two silicon atoms are equivalent. The O—Si—O bond angles around the two central silicon atoms are basically tetrahedral, but with a significant distortion in the case of the medium-sized vacancy, V_O^+(E), since the ring structure is not symmetric. In an attempt to locate a second minimum geometry for V_O^+(E), one of the silicon atoms was moved in a line though the three neighboring oxygen atoms and the energies calculated with the remaining atoms held fixed. The energies obtained are shown in **Figure 5**. The energies are found to rise rapidly as bonds are bent and shortened. Similar, but less dramatic rises in energy occur for the small cluster, V_O^+(C).

Since a "puckered" minimum energy configuration for V_O^+(E) did not arise naturally in our calculations, we sought such a configuration by carrying out a geometry optimization starting from a puckered configuration in which one of the central silicon atoms was placed within the oxide network while the remaining atoms were left at their locations within the optimized positive vacancy. The hope here was that if there were a bistable state, then starting the optimization in a state near the second local minimum would allow the system to converge to this other minimum. In this case, the silicon atom spontaneously moves back into the vacancy after only a few iterations of the geometry optimization suggesting that the dimer is the only locally stable minimum energy configuration. Boero and coworkers[27] have noted that this is the case when no suitable oxygen candidate is available to stabilize the puckered configuration.

In the case of the large positively charged vacancy model, V_O^+(G), the geometry is found to spontaneously distort with one silicon atom bonding to an oxygen atom in the network (**Figure 4c**), moving slightly over an angstrom from its original position toward one of the oxygen atoms in the surrounding network. The spin density is found to localize on the silicon atom remaining in the vacancy site. In **Table 7**, we estimate the stability of the large neutral, V_O^0(G), and positive, V_O^+(G), vacancies at their optimized configurations with respect to the removal and addition of an electron. We find an energy difference on the order of 3 eV for both neutral and positively charged vacancies at the two optimized configurations. No indication of a barrier between the two configurations was observed during the optimization.

DISCUSSION

The results presented here for the E'_δ center show excellent qualitative and quantitative agreement over the range of cluster sizes used. This suggests that (a) further extension of the cluster size will have little effect on the spin properties, and (b) a reasonable size cluster can accurately provide the spin properties of point defects in solids. The calculations on the model E'_δ structures suggest that the center detected in the ESR spectrum as a 100 G doublet could not involve distribution of unpaired electron spin over more than two Si atoms. In the case of the five-Si and four-Si atom model structures, the spin density is not calculated to be distributed equally. Moreover, the magnitude of the spin density calculated in these models (A and B) are incompatible with the observed spin properties for the E'_δ center.

The only model that seems plausible, on the basis of the calculated values of the spin properties, is a two-Si model. In this case, the Si atoms adjacent to the oxygen vacancy share most of the spin density and the wavefunction exhibits at least a 5:1 ratio of the *s* and *p* characters. The large *s* character of the wavefunction results in a reduced anisotropy in the hyperfine spectrum. These results, therefore, suggest that E'_δ center is a simple mono-oxygen vacancy involving two Si atoms.

The calculated results for the triplet-state center do not agree, either in a two-Si atom or in a four-Si atom model, with the experimental results for a triplet species. There are a number of possible reasons for this discrepancy between the theory and experiment. (1) The observed triplet-state spectrum may result from a species whose identity remains unknown. (2) The triplet state center may involve excess Si, but with a microscopic structure different from that of the E'_δ center. (3) The theoretical treatment used in the

present study may not be adequate for characterizing a triplet state. At this moment, however, the origin of the triplet-state spectrum in the ESR spectrum of the irradiated *a*-SiO_2 samples remains unresolved.

Formation mechanism of oxygen vacancy centers

We believe that a clearer picture of the mechanism of formation of neutral and positively charged oxygen vacancies emerges from our work. It is first noted that in all cases, the relaxation of the network following the removal of a neutral oxygen atom results in the formation of a Si—Si dimer bond between the two Si atoms adjacent to the oxygen vacancy site. The two Si atoms move inward from their initial positions in the precursors. (Models D, F, and H.) The calculated Si—Si bond in V_O^0 is somewhat larger in model H which may be due to the use of a relatively poor basis set. This observation is consistent with previous semi-empirical and *ab initio* calculations.[1,26,34]

Trapping of a hole by the neutral oxygen vacancy site in all three clusters results in a lengthening of the Si—Si bond distance relative to that of the relaxed neutral vacancy, V_O^0. Upon placing a positive charge on the vacancy, the two Si atoms in the case of models D and F move slightly away from each other. However, the Si—Si distance in both cases D and F is still about 0.3Å to 0.5Å shorter than prior to the formation of the vacancy. In contrast, a density functional theory [DFT] calculation in supercell approximation[27] suggests that the Si atoms adjacent to V_O^{+1} always "move away" from the vacancy, i.e., the Si—Si distance is always greater than the Si—Si distance prior to the formation of the vacancy. We consider this result of Ref. [27] to be wrong, and perhaps caused by the approximations used in the calculation. The reason for this is not apparent to us, however, it is clear that the method used by these authors is incapable of adequately describing a localized charged defect in amorphous material. In fact, Boero *et al*[27] also obtain an

incorrect description of the equivalent defect in the crystalline SiO_2 (quartz), where the Si—Si bond length in the case of V_O^{+1} is nearly the same as prior to the vacancy formation.

Unlike model D and F, the cluster in model H relaxes asymmetrically upon placing a positive charge on V_O^0. (Model I) The corresponding increase in R (Si—Si) in the case of asymmetric relaxation, V_O(C), is over 1.3Å. We note that one of the Si atoms adjacent to V_O moves away from its original position in the V_O^0 to a position inside the network to form a weak bond with a nearby O atom. The spatial location of this O atom, which is pointing inside one of the six-member rings, facilitates the puckering of the system.

In model D (=V_O(C)) with no rings beyond the second nearest-neighbor O atoms (with respect to the missing bridging oxygen) and in model F (=V_O(E)) with two 6-atom fused rings on each side of V_O^0, the lengthening of the Si—Si bond following hole trapping is accompanied by a shortening of the Si - second nearest neighbor oxygen bond lengths by about 0.4-0.5Å. However, in the case of V_O(G) with two 12 atom fused rings on each side of V_O, there is only a marginal change of the Si - second nearest neighbor -O bond distance for the undistorted side of the cluster around V_O after hole trapping. On the other side of the cluster, a Si atom spontaneously moves away from its position, and forms a weak bond with a three-fold coordinated O center. After hole trapping, the bond length between the Si (moved) and second nearest neighbor O atom (2^{nd} NN-O) increases to a value of about 1.76Å. One of the 2^{nd} NN-O - Si (moved) - O angles decreases from about 110° to about 99° while the other two angles deform only slightly. The reason for this change in behavior may be easily understood by analogy with ring formation in basic carbon chemistry where it is well known that six atom rings are the most stable, i.e. minimally strained, configuration. In the case of the positively charged vacancies we have studied, the medium

sized vacancy, $V_O(E)$, is already in a six atom ring configuration and can only distort by forming a four atom ring structure. On the other hand, the large positively charged vacancy, $V_O(G)$, forms a six-atom ring structure when it deforms.

Interestingly, the energy of formation of the positively charged vacancy, $\Delta E_f(V_O^+)$, with respect to V_O^0 [**Table 6**] is calculated to be about 1.1 eV higher in the case of model $V_O(E)$ than that in $V_O(C)$. However, the value of $\Delta E_f(V_O^+)$ in both $V_O(C)$ and $V_O(E)$ is substantially larger, by a factor of 2.5-3 than that in the case of model cluster $V_O(G)$. In fact, $\Delta E_f(V_O^+)$ at the V_O^0 optimized geometry is calculated to be only 2.83 eV [**Table 7**]. Such a low value of $\Delta E_f(V_O^+)$ in the case of model cluster $V_O(G)$ indicates the ease with which an asymmetrically relaxed deep hole trap (E'_γ) is formed in an oxide network with highly flexible structures.

One also notes that the electron affinity (vertical attachment) of V_O^+ (asymmetric) at its optimized geometry is about 0.7 eV higher than the vertical ionization potential of V_O^0, suggesting that the former is a deep trap center.

CONCLUSIONS

Charge trapping by oxygen vacancy defects in *a*-SiO_2 plays a critical role in determining the electrical properties of thin film semiconductor devices. A microscopic understanding of the structure of these vacancies and as well as the structural changes that accompany charge trapping are essential for improving our fundamental understanding of MOS device physics. We have presented the results of our *ab initio* HF calculations of structure and spin properties of model clusters representing E'_δ and the triplet-state centers observed in the ESR spectra of *a*-SiO_2. The calculations were able to rule out the five-Si

and four-Si atom models, which require multiple oxygen vacancies, as possibilities for the local atomic structure of the E'_δ center. The electronic structure and the spin properties of the two-Si atom model involving a simple mono-oxygen vacancy are calculated to be in close agreement to the experimental results for the E'_δ center. These calculated results are also in excellent agreement with our previous study on the E'_δ center using smaller model clusters. Therefore, we believe that E'_δ centers involve a trapped hole on two equivalent Si atoms adjacent to a mono-O vacancy. The two-Si atom model, however, does not seem to be a plausible structure for the triplet-state centers observed with the E'_δ centers in the ESR spectra of irradiated *a*-SiO_2. The calculated results also do not favor a four-Si atom model for the triplet state.

Our results suggest that the energy of formation, ΔE_f, of V_O^0 and V_O^{+1} depend upon the starting size and geometry of the precursor. The value of ΔE_f for V_O^0 and V_O^{+1} decreases with the flexibility and asymmetry in the oxide network.

They also suggest that microscopic structural changes due to hole trapping by V_O^0, primarily network relaxation, strongly depend on the local structure around the vacancy before the hole is trapped. A neutral vacancy, V_O^0, tends to form a Si—Si dimer bond regardless of the network structure. Similarly, hole trapping at a neutral oxygen vacancy in a relatively rigid network containing 6-atom (3-membered) fused rings results in a small, but symmetric relaxation (i.e., elongation) of the Si—Si bond at the vacancy site. When the network contains more flexible structures, such as 12-atom (6-membered) rings adjacent to the oxygen vacancy site and possesses sufficient asymmetry, trapping of a hole causes an asymmetric relaxation of the two adjacent Si atoms. The asymmetric relaxation in our calculation proceeds without a barrier.

These calculations would not have been possible without access to significant computational resources.

Acknowledgements

We would like to thank Dr. Prakashan Korambath, Dr. Rod Devine, Prof. Henry Kurtz, and Prof. Gianfranco Pacchioni for helpful discussions. We would also like to thank the University of New Mexico (UNM) for access to the resources of their Albuquerque High Performance Computing Center (AHPCC) and Maui High Performance Computing Center (MHPCC). The calculations on the small and medium-sized clusters were performed using IBM SP2 and SGI Origin 2000 at AHPCC, MHPCC, and the Aeronautical Systems Center/Major Shared Resource Center (ASC/MSRC). The calculations on the large-sized clusters were performed utilizing the UNM-Alliance Roadrunner Supercluster located at AHPCC under Grant Number 1999022.

TABLES

Table 1. General computational requirements for this series of studies. For models H and I, the times listed are those for the geometry optimizations of the neutral and positively-charged species starting from the optimized precursor configuration. In cases where different numbers of processors were used for a series of calculations, the most commonly used number of processors is indicated in parentheses.

Model	# of Atoms	Basis Set	# of Basis Functions	# of Processors	Runtime (Hours)	Total CPU Hours	Platforms used
A	29	DZP	360	1-8 (8)	96.9	500.1	IBM, SGI
B	28	DZP	336	8	120.5	964.0	IBM, SGI
E	39	DZP	557	8-32	673.0	3634.5	IBM, SGI
F	38	DZP	542	3-32 (8)	1013.2	7391.6	IBM, SGI
G	87	STO-3G	395	8-32 (24)	264.85	7133.6	IBM, Linux
H[a]	86	STO-3G	390	32	4.933	157.9	Linux
I[b]	86	STO-3G	390	32	4.44	142.3	Linux

[a] 91 Geometry Iterations, 727 SCF Iterations.

[b] 64 Geometry Iterations, 715 SCF Iterations.

Table 2. ^{29}Si spin properties in two-Si atom model cluster. Si_1 and Si_2 refer to the Si atoms adjacent to V_O. [From Reference 3.]

Center	ρ^0	a_{iso}(G)	T_{11}(G)	T_{22}(G)	T_{33}(G)
Basis set I[a]					
Si_1	0.219676	-69.69	11.06	9.15	-20.21
Si_2	0.242067	-76.80	11.66	10.08	-21.74
Basis set II[b]					
Si_1	0.326490	-103.58	9.27	8.63	-17.90
Si_2	0.372170	-118.07	9.88	9.58	-19.46
Expt, Ref.[11,25]		100			

[a]STO-3G. Calculated total energy, E = -3768.141957 Hartree.
[b]DZP. Calculated total energy, E = -3814.852743 Hartree.

Table 3. Calculated ^{29}Si spin properties for the triplet-state center. [From Reference 3.]

Configuration	Precursor	Optimized
R(Si—Si) (Å)	3.0894	4.0435
E (Hartree)	-1030.788045	-1030.843963
ρ^0	1.692381	1.294420
a_{iso} (G)	-536.92	-410.66
T_{11} (G)	25.46	21.77
T_{22} (G)	25.23	21.32
T_{33} (G)	-50.69	-43.08

Table 4. Structural parameters adjoining vacancy site for RHF calculations on precursor clusters.

Model cluster	**C**[a]	**E**[b]	**G**[b]
$R_{Si—Si}$(Å)	3.089	3.119	3.077
$R_{Si—O}$(Å) (adjoining center)	1.625	1.623-1.638	1.583-1.624
$R_{Si—O}$(Å) (all)	1.621-1.624	1.603-1.646	1.583-1.697
Si—O (central)—Si bond angle	170°	153.740°	146.182°
E (Hartree)	-1105.961598	-3891.533817	-7909.281697
Basis Set	DZP	DZP	STO-3G

[a] Reference 1.
[b] Reference 4.

Table 5. Structural parameters adjoining vacancy site for RHF calculations on optimized neutral vacancies. [From Reference 4.]

Model Vacancy (V_O)	**V_O^0(C)**	**V_O^0(E)**	**H=V_O^0(G)**
$R_{Si—Si}$(Å)	2.351	2.331	2.438
$R_{Si—O}$ (Å) (adjoining center)	1.635	1.6334-1.6504	1.608-1.641
$R_{Si—O}$ (Å) (all)		1.604-1.6504	1.587-1.696
O—Si(1)—O bond angles		104.510°	108.714°
		109.794°	107.045°
		103.706°	106.982°
O—Si(2)—O bond angles		108.778°	105.542°
		104.001°	107.630°
		104.507°	108.555°
E (Hartree)	-1030.950265	-3816.521002	-7835.368618
Basis Set	DZP	DZP	STO-3G

Table 6. Important structural parameters for UHF calculations optimized positively charged vacancies.

Model positive vacancy (V_O^+)	**D=V_O^+(C)[a]**	**F=V_O^+(E)[b]**	**I=V_O^+(G)[b]**
$R_{Si—Si}$(Å)	2.798	2.650	3.766
$R_{Si(1)—O}$ (Å) (# of atoms)	1.587	1.582-1.604 (3)	1.624-1.646 (3)
$R_{Si(2)—O}$ (Å) (# of atoms)	1.587	1.588-1.602 (3)	1.561-1.759 (4)
$R_{Si—O}$ (Å) (all)	n/a	1.582-1.681	1.561-1.759
O—Si (1)—O bond angles		110.812° 118.676° 109.662°	106.384° 107.028° 107.722°
O—Si(2)—O bond angles		117.434° 110.328° 110.613°	113.946° 115.787° 99.555° 115.848° 105.908° 103.068°
$\rho^0_{,Si(1)}$, $\rho^0_{,Si(2)}$	0.2740, 0.2730	0.3016, 0.3214	0.4380,-0.0005
E (Hartree)	-1030.662080	-3816.193912	-7835.252629
E-E(V_O) (eV)	7.8421	8.9007	3.1563
Basis Set	DZP	DZP	STO-3G

[a] Reference 1.
[b] Reference 4.

Table 7. Energy changes associated with relaxation after adding or removing an electron from the neutral and positively charged large vacancies (model $V_O(G)$) at their respective optimized configurations at the STO-3G level. [From Reference 4.]

Structure	Energy (Hartree)	Relative Energy, $E-E_{opt}$ (eV)
V_O^+ at V_O (opt. geometry)	-7835.148516	2.8331
V_O at V_O^+ (opt. geometry)	-7835.238161	3.5500

FIGURES

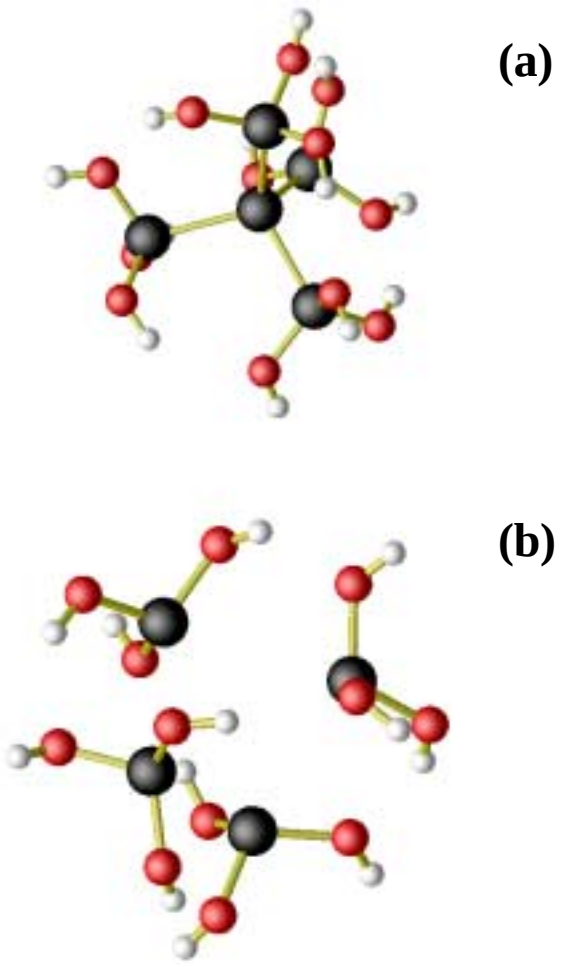

Figure 1. (a) Model A. A precursor cluster model representing a 5-Si center vacancy site, i.e. a Si island. (b) Model B. Derived from model A by removing the bridging O atom, it represents a four-center vacancy site.

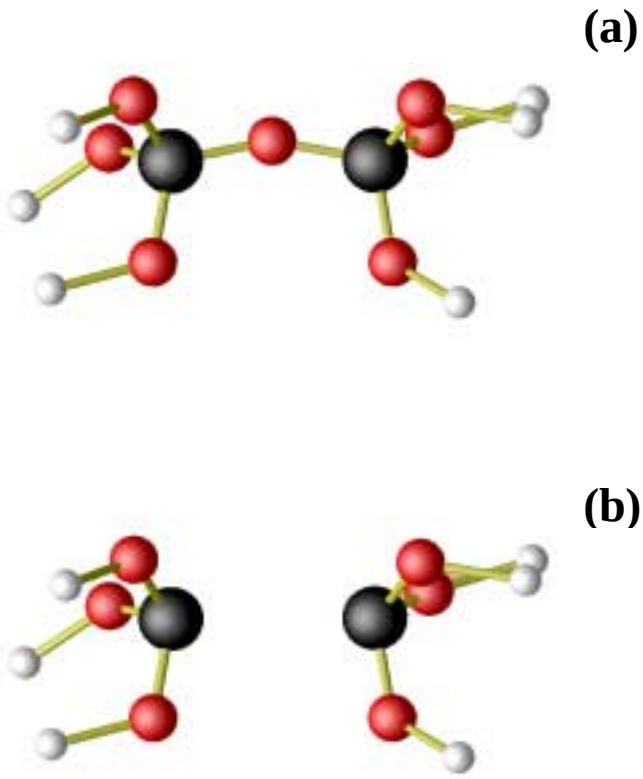

Figure 2. (a) *Model C.* Shown is the optimized configuration for the 15-atom precursor cluster. The large black atoms are silicon atoms, the medium-sized red atoms are oxygen atoms, and the smallest white atoms are hydrogen atoms. Bonds are shown for bond orders greater than 0.5. (b) *Model D.* A model for a 2-Si center mono-oxygen vacancy site obtained from model C by removing the bridging O atom.

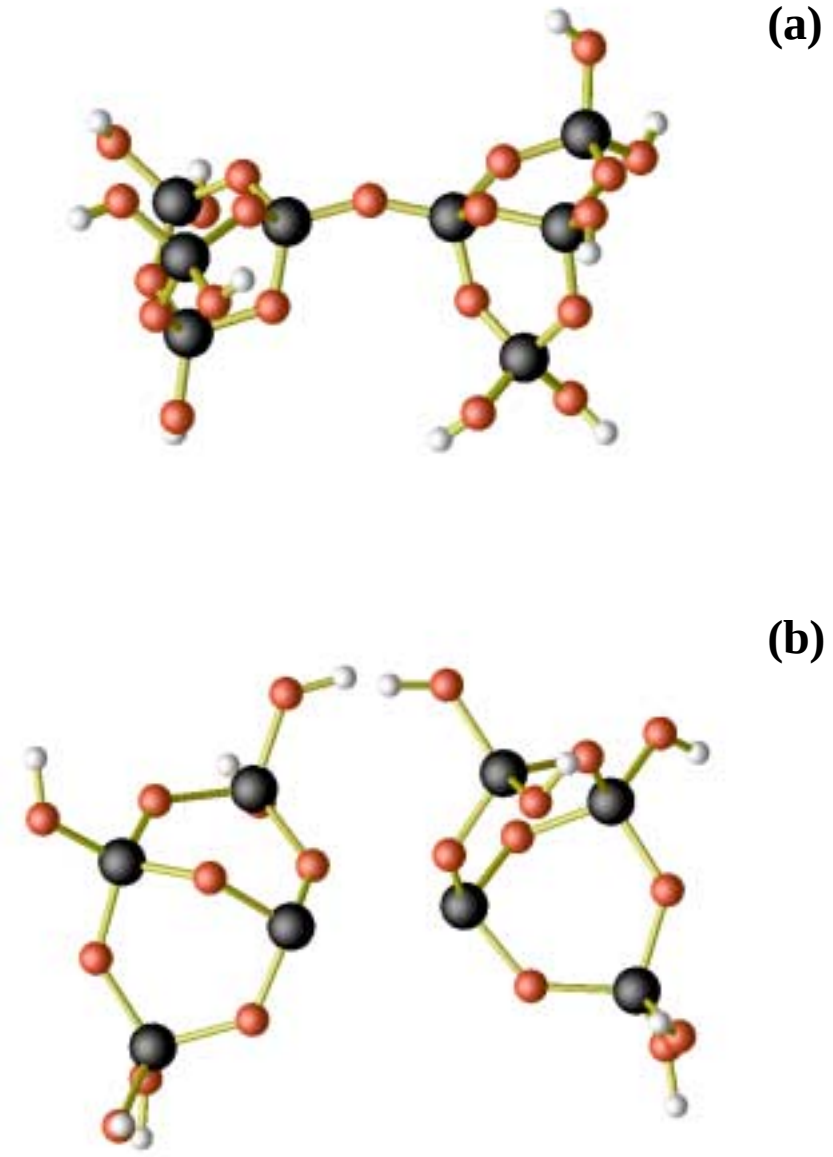

Figure 3. (a) *Model E.* Shown is the optimized configuration for the 39-atom precursor cluster. The large black atoms are silicon atoms, the medium-sized red atoms are oxygen atoms, and the smallest white atoms are hydrogen atoms. Bonds are shown for bond orders greater than 0.5. (b) *Model F.* Shown is the optimized configuration for the model 38 atom, neutral, 2-silicon center mono-oxygen vacancy, V_O. (V_O^0(E)) Bonds are shown for bond orders greater than 0.5, except between the central Si atoms, where it is omitted for clarity.

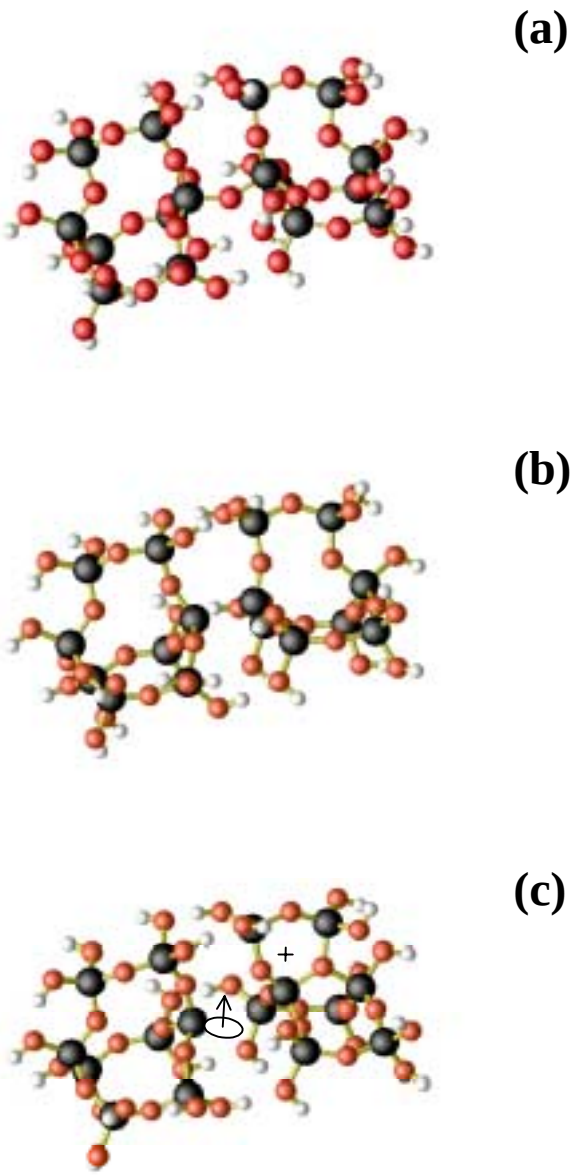

Figure 4. (a) *Model G.* Shown is the optimized configuration of the 87-atom precursor cluster. The large black atoms are silicon atoms, the medium-sized red atoms are oxygen atoms, and the smallest white atoms are hydrogen atoms. Bonds are shown for bond orders greater than 0.5. (b) *Model H.* Shown is the optimized configuration for the 86-atom, neutral, 2-silicon center mono-oxygen vacancy, V_O. (V_O^0(G)) Bonds are shown for bond orders greater than 0.5. (c) *Model I.* Shown is the optimized configuration for the 86-atom, positively charged, 2-silicon center mono-oxygen vacancy, V_O^+. (V_O^+(G)) Note that one of the central silicon atoms has migrated outward and bonded to an oxygen atom in the outer network.

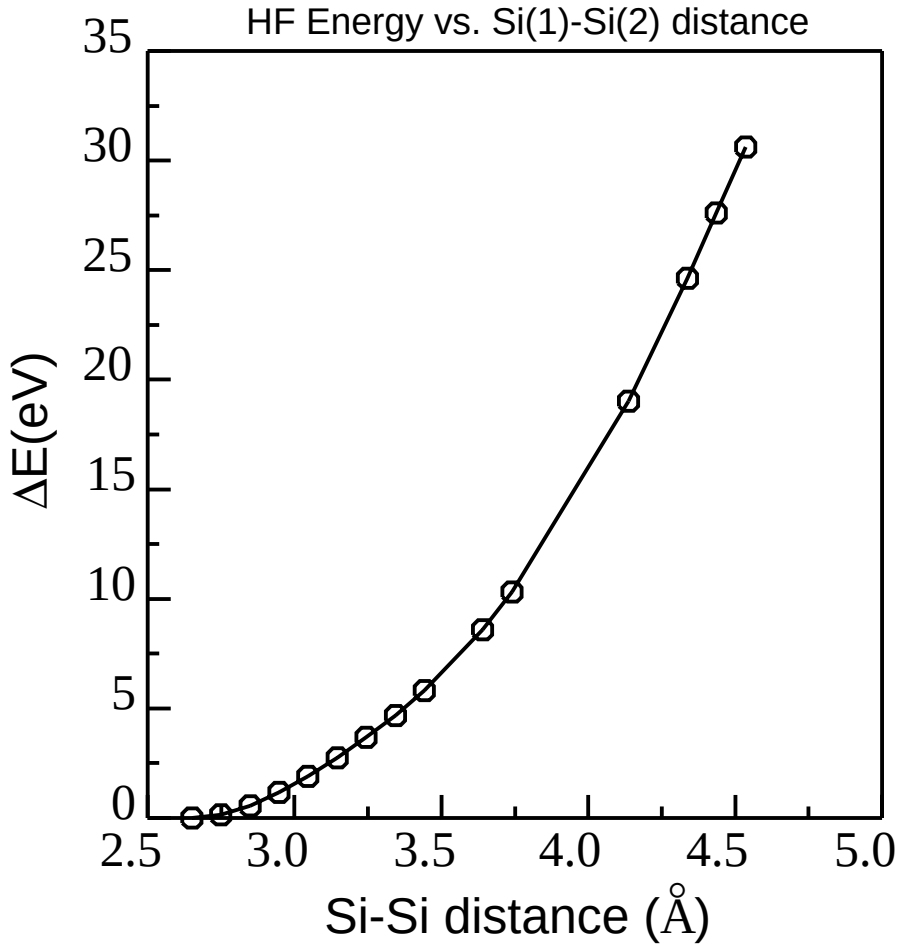

Figure 5. Hartree-Fock Energy vs. Si(1)-Si(2) distance as Si(1) is distorted outward from its equilibrium position in the model positively charged, 2-silicon center, mono-oxygen vacancy, $V_O^+(E)$. The remaining atoms are held fixed. The lines in the figure are guides to the eyes.

REFERENCES

[1] Chavez, J.R.; Karna, S. P.; Vanheusden, K.; Brothers, C. P.; Pugh, R.D.; Singaraju, B.K.; Devine, R.A.B. *IEEE Trans. Nucl. Sci.*, **1997**, *44*, 1799.

[2] Feigl, F.J.; Fowler, W. B.; Yip, K. L. *Solid State Commun.*, **1974**, *14*, 225.

[3] Karna, S. P.; Pineda, A. C.; Shedd, W.M.; Singaraju, B.K. *Silicon-on-Insulator Technology and Devices IX (Proceedings Volume 99-3)*, Hemment, P. L. F., Ed.; The Electrochemical Society: Pennington, NJ, **1999**,161.

[4] Pineda, Andrew C.; Karna, Shashi P. *J. Phys. Chem. A* **2000**, *104*, 4699.

[5] Weeks, R. A. *J. Non-Cryst. Solids*, **1994**, *179*, 1.

[6] Griscom, D.L. *Nucl. Instr. Methods B,* **1984**, *1*, 481.

[7] Devine, R. A. B. *Jp. J. Appl. Phys.*, **1992**, *31*, 4411.

[8] Devine, R. A. B. *IEEE Trans. Nucl. Sci.*, **1994**, *41*, 452.

[9] Fleetwood, D.M.; Riewe, L.C.; Schwank, J.R.; Witzak, S.C.; Schrimpf, R.D. *IEEE Trans. Nucl. Soc*., **1996**, *43*, 2537.

[10] Fleetwood, D.M.; Winokur, P.S.; Riewe, L.C.; Reber, R.A., Jr. *J. Appl. Phys.*, **1998**, *84*, 6141.

[11] Griscom, D.L.; Frieble, E. J. *Phys. Rev.* B, **1986**, *34*, 7524.

[12] Lenahan, P. M.; Dressendorfer, P. V. *J. Appl. Phys.*, **1983**, *54*, 1457.

[13] Lenahan, P. M.; Dressendorfer, P. V. *J. Appl. Phys.*, **1984**, *55*, 3495.

[14] Rudra, J. K.; Fowler, W. B. *Phys. Rev. B.*, **1987**, *11*, 2327.

[15] Cook, M.; White, T. C. *Phys. Rev. Lett.*, **1987**, *59*, 1741.

[16] Snyder, K. C.; Fowler, W. B. *Phys. Rev. B*, **1993**, *48*, 13238.

[17] Tohmon, R.; Shimogaichi, Y.; Tsuta, Y.; Munekuni, S.; Ohki, Y.; Hama, Y.; Nagasawa, K. Phys. Rev. B., **1990**, *41*, 7258.

[18] Vanheusden, K.; Stesmans, A. *J. Appl. Phys.*, **1993**, *74*, 275.

[19] Warren, W. L.; Fleetwood, D. M.; Shaneyfelt, M. R.; Schwank, J. R.; Winokur, P. S.; Devine, R. A. B. *Appl. Phys. Lett.*, **1993**, *62*, 3330.

[20] Devine, R. A. B.; Mathiot, D.; Warren, W. L.; Fleetwood, D. M.; Asper, B. *Appl. Phys. Lett.*, **1993**, *63*, 2926.

[21] Conoley, Jr., J. F.; Lenahan, P. M.; Evans, H. L.; Lowery, R. K.; Morthorst, T. J. *Appl. Phys. Lett.*, **1994**, *65*, 2281.

[22] Devine, R. A. B.; Warren, W. L.; Xu, J. B.; Wilson, I. H.; Paillet, P.; Leray, J.-L. *J. Appl. Phys.*, **1995**, *77*, 175.

[23] Zvanut, M. E.; Chen, T. L.; Stahlbush, R. E.; Steigenwalt, E. S.; Brown, G. A. *J. Appl. Phys.*, **1995**, *77*, 4329.

[24] Conoley, J.F. Jr.; Lenahan, P.M. *IEEE Trans. Nucl. Sci.*, **1995**, *42*, 1740.

[25] Zhang, L.; Leisure, R.G. *J. Appl. Phys.* **1996**, *80*, 3744.

[26] Rudra, J.K.; Fowler, W. B. *Phys. Rev. B*, **1987**, *35*, 8223.

[27] Boero, M.; Pasquarello, A.; Sarnthein, J.; Car, R. *Phys. Rev. Lett.* **1997**, *78*, 887.

[28] Warren, W.L.; Lenahan, P.M.; Robinson, B.; Stathis, J.H. *Appl. Phys. Lett.* **1988**, *53*, 482.

[29] Zvanut, M.E.; Feigl, F. J.; Fowler, W.B.; Rudra, J.K.; Caplan, P.J.; Poindexter, E.H.; Zook, J.D. *Appl. Phys. Lett.*, **1989**, *54*, 2118.

[30] Warren, W.L.; Lenahan, P.M. *J. Appl. Phys.* **1989**, *66*, 5488.

[31] Schmidt, M. W.; Baldridge, K. K.; Boatz, J. A.; Elbert, S. T.; Gordon, M. S.; Jensen, J.H.; Koseki, S.; Matsunaga, N.; Nguyen, K. A.; Su, S. J.; Windus, T. L.; Dupuis, M.; Montgomery, J. A. *J. Comp. Chem.*, **1993**, *14*, 1347.

[32] Dupuis, M.; Farazdel, A.; Karna, S. P.; Maluendes, S. in *Modern Techniques in Computational Chemistry*, E. Clementi, Ed. ESCOM Science Publishing, Leiden, **1990**.

[33] Karna, S. P.; Grein, F. *Int. J. Quant. Chem.*, **1989**, *36*, 265; *Mol. Phys.*, **1992**, *77*, 135.

[34] Snyder, K.C.; Fowler, W.B. *Phys Rev. B*, **1993**, *48*, 13238.